Journal of Fluorescence, Vol. 14, No. 4, July 2004 (©2004)

Optical Detection of Thymine Dinucleoside Monophosphate and Its *cis-syn* Photodimer by Inorganic Nanoparticles

K. K. Caswell,[1] Rahina Mahtab,[2] and Catherine J. Murphy[1,3]

Received November 22, 2003; revised February 16, 2004; accepted February 16, 2004

The Watson-Crick DNA double helix is an averaged ideal of multitudinous natural sequence-directed local structural deviations. By effectively derailing normal cellular physiological processes, damaged bases can induce noncanonical irregularities in the local structure of DNA if not efficiently repaired. Pyrimidine bases, especially thymine, are prone to dimerization when exposed to ultraviolet light. A [2 + 2] photocyclo-addition between adjacent thymine bases predominantly produces the *cis-syn* photodimer. These lesions, implicated in skin cancer, bend DNA by $\sim 30^{\circ}$ due to their structural and conformational changes. Such changes in molecular properties can be detected by differential quenching of CdS nanoparticle luminescence and by surface-enhanced Raman scattering spectroscopy on metal nanoparticle substrates.

KEY WORDS: Thymine; photodimer; CdS; luminescence; SERS.

INTRODUCTION

The Watson-Crick double helix represents an averaged ideal of various natural sequence-directed local structural deviations. Disease-related lesions can induce noncanonical irregularities in the local structure of DNA that effectively derail normal cellular physiological processes if they are not efficiently repaired [1–7]. Pyrimidine bases, especially thymine, are prone to dimerization when irradiated with ultraviolet light [7–9]. A [2 + 2] photocycloaddition at bipyrimidine sites produces predominantly the *cis-syn* photodimer (Fig. 1). These lesions, through their structural and conformational changes, bend DNA by $\sim 30^{\circ}$ [7], present barriers to normal polymerase function through anomalous transcription and/or replication that induces cell death or proliferation, and have been implicated in skin cancer [7,8,10].

Many of the current methods (e.g., immunological assays, enzyme digestion/electrophoretic quantification, ligation-mediated polymerase chain reaction) used to detect these bipyrimidinic lesions are indirect and do not provide sufficient sensitivity to allow for discrimination among various photoproducts, and some suffer from calibration issues [9]. Isolation of UV-damaged DNA photoproducts, followed by high performance liquid chromatography (HPLC), in conjunction with electrospray ionization tandem mass spectrometry (MS/MS), has overcome the inability of other chromatographic methods (e.g., GC-MS) to simultaneously detect various photoproducts [9]. Ideal methods would be less time-consuming and destructive and have greater sensitivity and selectivity.

Nanoparticles have been used to detect both DNA sequences [11] and unusual DNA structures [12–17]. Semiconductor nanoparticles that are of comparable size and surface charge to proteins have been used as photoluminescent probes of DNA with intrinsic curvature [12–17]. Prior results have indicated that CdS luminescence quenching depends on the degree to which DNA adsorbates interact at the surface of 4 nm CdS particles [12–17]. This previous work also has demonstrated that "kinked" DNA binds with higher affinities and faster on-rates

[1] Department of Chemistry and Biochemistry, University of South Carolina, 631 Sumter Street, Columbia, Columbia, South Carolina 29208.

[2] Department of Physical Sciences, South Carolina State University, Orangeburg, South Carolina 29117.

[3] To whom correspondence should be addressed. E-mail: murphy@mail.chem.sc.edu

1053-0509/04/0700-0407/0

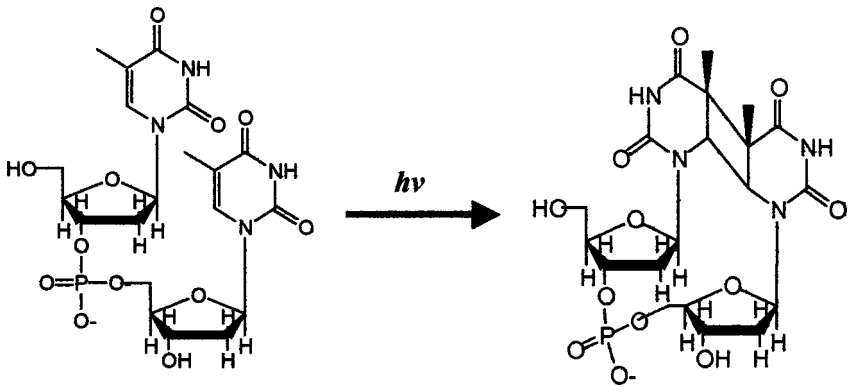

Fig. 1. UV-induced [2 + 2] photocycloaddition between adjacent thymine bases. The 5,6 double bonds of TpT (left) are reconfigured to form a butane ring, effectively fusing the 6-member rings of the bases together.

to spherical CdS surfaces than does normal "straight" DNA [12–16]. This tendency should lead to differential binding of the radically different structurally and conformationally influenced properties of otherwise similar molecules, such as thymine dinucleoside and its *cis-syn* photodimer.

However, though photoluminescence is a means of detection with great sensitivity, it does not provide the structural "fingerprint" information of Raman spectroscopy. Molecules adsorbed to metallic surfaces with nanoscale roughness (or curvature) classically experience enhancements of their Raman signals on the order of 10^3–10^6 by the surface-enhanced Raman scattering (SERS) phenomenon [18–24]. The major source of Raman signal enhancement in SERS is commonly attributed to the increased electric field at the metal surface upon visible light absorption, which is predicated on surface roughness (or curvature) and aggregation effects [18–28] (note that the latter is confined to colloidal systems). For silver and gold, the most common SERS substrates, visible light matches the collective oscillation of their conduction band electrons, inducing a dipole moment and a surface plasmon. Of the SERS-active substrates, colloidal silver offers the advantages of the greatest enhancements and ease of preparation [18–28]. Enhancements in excess of 10^{14}, compared with the inherently weak sensitivity of "normal" non-resonant Raman scattering, have been achieved with single molecule detection configurations [24–28]. Therefore, SERS spectroscopy shows the potential of providing sensitivity that approaches that of fluorescence while providing a structural "fingerprint" and orientational information of the adsorbate at the nanoparticle surface [24–29]. These attributes are proving invaluable tools in biomedical research [18,19,25,29], and therefore, SERS seems a likely tool to investigate DNA lesions.

In addition, as a tool for biomedical spectroscopy, SERS shows great promise for various applications, including probing of lipid chemistry, neurotransmitters, membrane transport processes, enzyme immunoassays, and DNA [25]. Thus far, the studies that have employed SERS to investigate DNA have focused primarily on its free bases and long polymers. We have recently used SERS to examine the influence of local DNA structures on the ability of the biopolymers to bind to Au nanoparticles [29]. Thymine dinucleoside monophosphate (TpT), an example of a bipyrimidinic site and precursor to a *cis-syn* thymine dimer photolesion, is a weak Raman scatterer, even in the crystalline form. By combining the sensitivity of photoluminescence with the structural and orientational information of SERS, disease-associated DNA lesions can be more thoroughly investigated.

EXPERIMENTAL

Materials

Anhydrous Na_2S (Alfa), $Cd(NO_3)_2{\cdot}4H_2O$ (Aldrich), sodium polyphosphate (average chain length of 18, Sigma), acetophenone 99% (Aldrich), methanol HPLC grade (Fisher), ammonium hydroxide (Fisher), formic acid (Fisher), sodium hydroxide (Fisher), sodium borohydride (Aldrich), silver nitrate (Aldrich), ascorbic acid (Aldrich), potassium chloride (EM Science, NJ), and acetonitrile (Fisher) were used as received from the manufacturers.

TpT was obtained from MWG Biotech Inc. (High Point, NC) and Genemed (South San Francisco, CA). All TpT, which was guaranteed pure and free of salt from the manufacturers, was dissolved in deionized

water (Water and Power Technologies Inc.) and filtered through 0.45 μm Millipore Ultrafree Microcentrifuge filters (Sigma).

Instrumentation

A 1000-W, short arc, xenon lamp (3.77×10^{-5} eins/min) was used (lamp housing Oriel model 66021 and power supply Oriel model 68820). A Beckman System Gold HPLC (32 Karat software package on an IBM computer) with a UV/Vis absorption detector module, using a Hamilton PRP-1 reversed-phase column, was employed for purification. Samples were dried on a ThermoSavant AES 1010-120 Speedvac system.

For verification and characterization, ^{1}H NMR (Varian Mercury 400 MHz), circular dichroism (CD; Olis RSM 1600, Cary-16 spectrophotometer/circular dichroism module, On-Line Instruments Inc.), tandem mass spectrometry (MS/MS; MicroMass Q-TOF [Quadrupole-Time of Flight] electrospray ionization), and absorption spectra were obtained with a Varian Cary 500 Scan UV-vis-NIR spectrophotometer. In addition, transmission electron microscopy (TEM) using a Hitachi H-8000 Electron Microscope (Tokyo, Japan) utilizing nitrocellulose grids provided detailed images of the CdS and Ag colloids.

Photoluminescence spectra were determined using an SLM-Aminco 8100 spectrofluorometer, with excitation at 350 nm and a 4 nm band pass. A Detection Limit Solution 633 Raman system was used for the SERS.

Procedures

The *cis-syn* photodimer was synthesized by using acetophenone as a photosensitizer. The TpT solution to be irradiated with UV light was prepared as follows: Deionized water was added to TpT to achieve ~1 mM concentration ($\varepsilon = 7400$ L·mol^{-1}·cm^{-1}) in a 50 mL round bottom flask, acetophenone was added at a 20:1 ratio to TpT, and finally, 10% methanol was added. This solution was sparged with N_2 for 40 minutes. A Teflon stir bar was used for gentle agitation. Finally, the solution was irradiated for ~2.5 hr at a distance of 1.5 feet from a 1000-W, short arc, xenon lamp. Light was passed through a Pyrex water filter to simulate the solar spectrum [30]. Every 15 min, aliquots were drawn to monitor the reaction. The aliquots were analyzed using reversed-phase HPLC on a column that had been cleaned and equilibrated with 100% 25 mM ammonium formate buffer (pH 7). The clean method was composed of 100% acetonitrile for 15 min adjusted on a linear gradient over 5 min to 100% H_2O for 10 min. The column was then reequilibrated to 100% 25 mM ammonium formate for 30 min. The composition of the mobile phase immediately (0.1 min) was altered to 5% methanol for 10 min. From there, it was increased to 50% methanol in 6 min linear gradient.

The *cis-syn* dimer elutes between 3–4 min, whereas unreacted TpT elutes between 15–16 min. Acetophenone does not elute at all in these conditions. Approximately 5 min into the clean method, the acetophenone begins eluting.

Irradiation was terminated once a plateau at which no more TpT appeared to be dimerizing had been achieved, typically ~2.5 hr. The solution was concentrated to ~1 mL on the Speedvac, then purified and characterized using the previously mentioned HPLC system and method. The collected fractions were dried and washed with deionized water three times, then rehydrated with deionized water.

The *cis-syn* thymine dimer was verified and characterized by ^{1}H NMR [31], MS/MS [9], circular dichroism [32], and absorption spectroscopy [8].

Following methods described in previous research, Cd(II)-activated CdS nanoparticles that were 4.5 nm in diameter and surface-enriched with Cd(II) were synthesized as a colloidal dispersion in water [13]. Nanoparticles were characterized using TEM for particle sizing, as well as absorption and photoluminescence spectroscopies.

Photoluminescence titrations were performed by adding 5 μL aliquots of 5 mM TpT to 300 μL of a 2×10^{-4} M (Cd) Cd(II)-CdS solution. Emission spectra were acquired 20 min after each DNA aliquot was added, which provided enough time to ensure that equilibrium was achieved [13]. Blank titrations of deionized water, without DNA, also were performed and used to correct the data for subsequent analyses.

Silver particles were synthesized according to a method adapted from Schneider *et al.* [33]. A 10 mL aqueous solution containing 1 mM NaOH, followed by 0.1 mM $NaBH_4$ and subsequently 10 mL of a 0.6 mM $AgNO_3$ solution, were combined with vigorous stirring. After the solution turned yellow, stirring continued for 2–3 min. Subsequently, 10 mL of 0.3 mM $AgNO_3$ was added very slowly to a 20 mL solution containing 0.25 mM NaOH, 0.15 mM ascorbic acid, and 0.3 mL of the yellow Ag solution with concomitant stirring. Immediately, 1 mL of 100 mM KCl was added for stability. The solution color was a pale yellow to peach color.

The Ag colloids were characterized using electronic absorption spectroscopy. All spectra show an absorbance maximum at 400 nm, typically with an absorbance of ~1.0. The particle size was measured by TEM. The samples were prepared for TEM by placing a 2 μL drop of a 10:1 dilution of deionized water to Ag colloid ratio on a 0.5 cm carbon-coated copper grid and allowing it to dry.

Particle sizes measured from TEM images averaged 44 nm in diameter.

The estimated concentration of nanoparticles was determined by calculating the total number of Ag atoms in the starting solutions and then determining how many atoms would constitute an average sized particle. The volume of a sphere that would correspond to the resultant average particle size was calculated, and the total number of atoms that would fit into each volume was determined using the crystal structure of Ag (cubic-unit cell = 408.53 pm on edge, 4 Ag atoms/unit cell), thus providing the average number of atoms per particle. The number of particles in each sample was calculated by dividing the total number of Ag atoms by the atoms per particle and then converting that to the number of moles of particles per L.

SERS was performed on a Raman system that uses a fiber optic probe equipped with a microscope objective to focus radiation from a 632.8 nm HeNe laser (25 mW laser power at the sample) on to the sample and collect the 180° Raman backscatter. Integration times were 240 s for each sample measured. Spectral acquisition and processing were enabled with DLSPEC and GRAMS/32 (Galactic Industries) software. KCl was the aggregating salt. A final concentration of 7×10^{-5} M of TpT or *cis-syn* dimer was achieved by adding a sufficient amount of TpT or *cis-syn* dimer to 2 μL of 1 M KCl and 200 μL of Ag colloids in a black-sided quartz cuvette.

RESULTS AND DISCUSSION

The *cis-syn* thymine dimer (Fig. 1) was produced by a photosensitized reaction of TpT using acetophenone. By using a photosensitizing reaction and irradiating at the upper end and outside the absorbance range of thymine, radical chemistry byproducts were avoided, and the *cis-syn* dimer yield was maximized. Performing this reaction under nitrogen using a 20:1 ratio of acetopheone to TpT and a 10% methanol composition provided similar benefits; it enhanced the desired product yield and reduced undesirable intermediate byproducts. To avoid intermolecular dimerization, the TpT solution concentration was diluted to 1 mM. This mixture reached a product plateau at ~2.5 hr of UV irradiation, according to reversed-phase HPLC monitoring (see the Experimental section). Figure 2 shows HPLC chromatograms that reveal where the photoproduct elutes relative to unreacted TpT. This disparity in elution times, given the setup parameters, is a strong indication of their relative polarities. Photodimer yields were typically ~70%–80%.

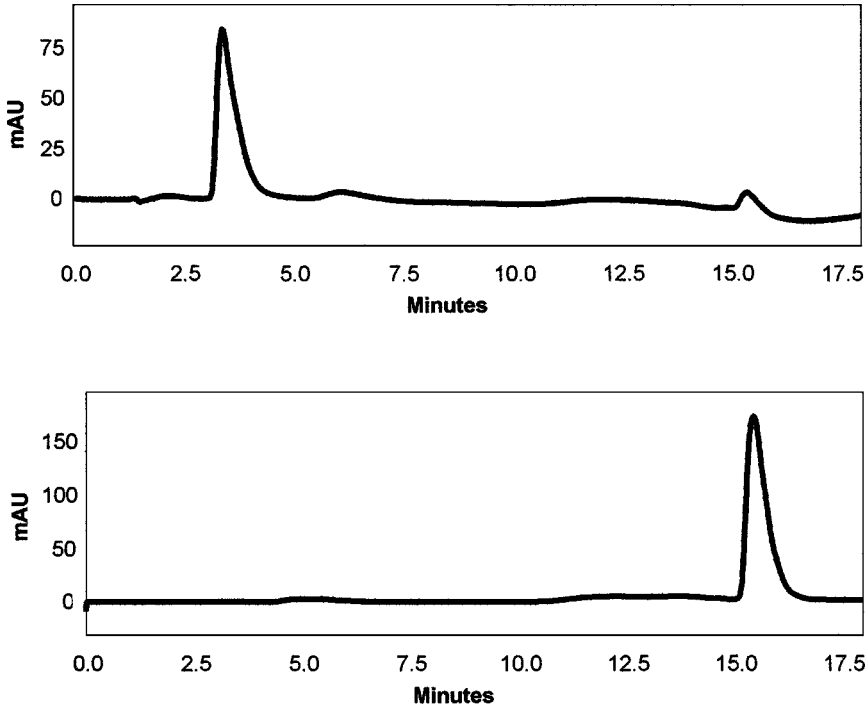

Fig. 2. HPLC chromatograms showing TpT at $t = 0$ (top) and at $t = 2$ hr (bottom) after ultraviolet irradiation.

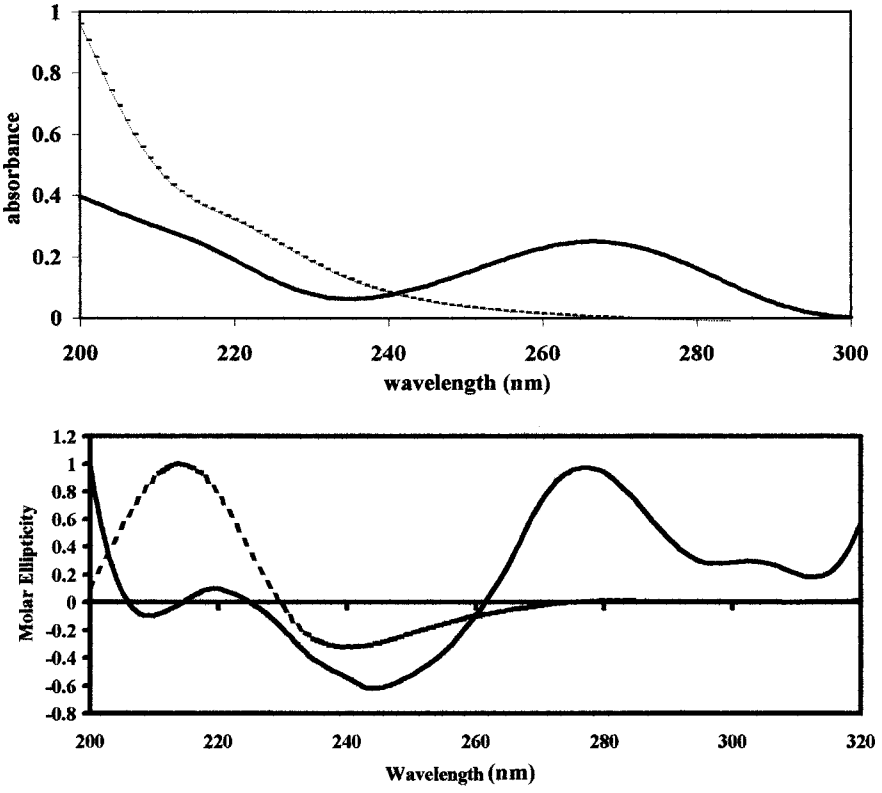

Fig. 3. UV-vis (top) and circular dichroism (bottom) spectra of TpT (solid line) versus *cis-syn* dimer (dashed line).

Verification and characterization of the photodimer product was as described in the Experimental section. For MS/MS, though the molecular weights are the same with a parent ion at $m/z = 545$, the fragmentation patterns are different for the dimer of interest with a daughter ion at $m/z = 447$ [9]. Because the 5,6 double bond is broken in a naturally occurring thymine ring and contributes to the butane ring formation between adjacent thymine bases, the UV absorbance maximum is no longer observed at ~265 nm [8]. Instead, there is a shoulder around 224 nm (Fig. 3, top). Circular dichroism corroborates the photodimer's molecular rearrangement relative to TpT (Fig. 3, bottom).

We have previously shown that CdS nanoparticles are photoluminescent, and this photoluminescence is sensitive to DNA adsorption [12–17]. The photoluminescence spectra (Fig. 4) were compared for the results of titrations of separate 300 μL solutions of Cd(II)-rich CdS nanoparticles with 35 μL of water, TpT, and its photodimer. The peak maximal intensity decrease of the 460 nm emission band with respect to DNA concentration also was monitored (Fig. 5).

The mechanism of nanoparticle photoluminescence quenching is not entirely well understood, but it is reversible with salt [16] and results in no permanent base damage after irradiation [13]. Therefore, we consider the nanoparticle–DNA interaction a simple donor-acceptor adduct, common in inorganic chemistry. The loss of the surface-associated Cd^{2+} is one likely source of quenching. Studies with double-stranded DNA have suggested that counterion release from the nanoparticle–DNA interface is the thermodynamic driving force of the interaction

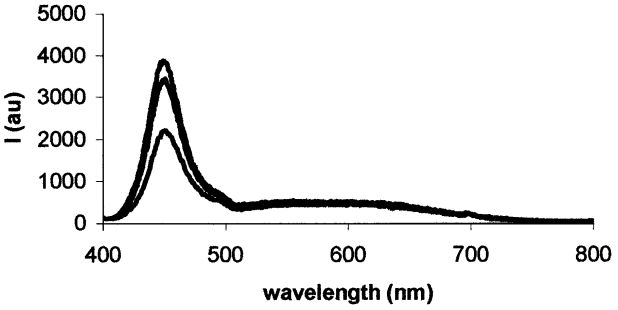

Fig. 4. Overlaid photoluminescence spectra of 300 μL of 2×10^{-4} M Cd(II)-rich CdS nanoparticles after addition of 35 μL of water (top), 35 μL of 5 mM TpT (middle), and 35 μL of 5 mM *cis-syn* photodimer (bottom) to separate equal-volume solutions.

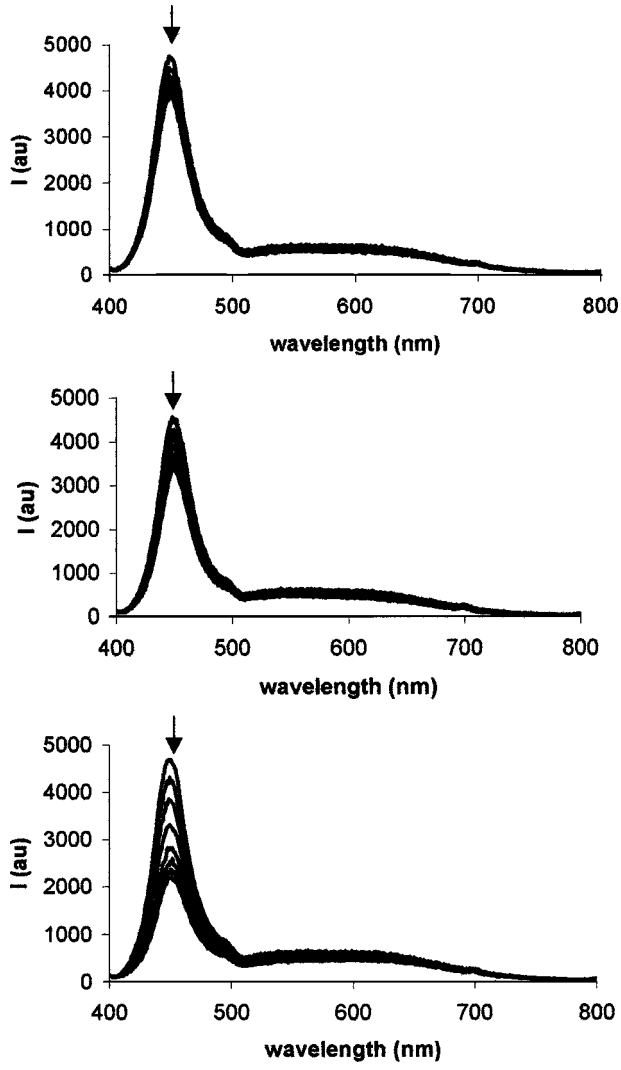

Fig. 5. Titrations of 300 μL CdS with 5 μL aliquots, for a total of 35 μL of deionized water (top), 5 mM TpT (middle), and 5 mM *cis-syn* dimer (bottom).

[16]. Titrations of cadmium-activated CdS nanoparticles with TpT reveal a marginal increase in ability to quench the luminescence over a water control (Figs. 4 & 5, top and middle). Whereas the photodamaged dimer did not quench the luminescence completely, it provided substantial quenching in comparison (Fig. 5, bottom). This finding is likely due to the dimer's increased polarity, as evidenced by its early elution at ~3 min on a reversed-phase column. In comparison, TpT requires ~16 min and some mobile phase coaxing.

The Langmuir adsorption isotherm was used to extract the relative binding constants for TpT and its photodimer product to the Cd(II)-CdS surface. This model is based on the assumptions that there is one molecule bound

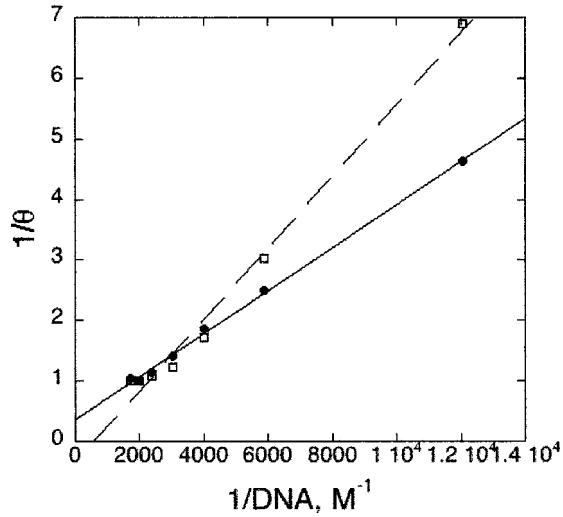

Fig. 6. Double-reciprocal plot of the CdS-DNA titration data, according to Langmuir adsorption isotherm. The reciprocal slope equals the binding constant K. • TpT ($K = 2800$ M^{-1}); □ *cis-syn* photodimer ($K = 1700$ M^{-1}).

per surface binding site (monolayer coverage), all binding sites on the surface are the same and fixed in number, and there are no interactions between molecules at the surface [34].

$$\theta = K[A]/(1 + K[A])$$

A double-reciprocal plot, $1/\theta$ vs. $1/[A]$, where $[A]$ is either the concentration of TpT or the dimer, should ideally be linear with a slope of $1/K$ and an intercept of one. Plotting the titration data, we found $K_{\mathrm{TpT}} = 2800$ M^{-1} and $K_{\mathrm{dimer}} = 1700$ M^{-1} (Fig. 6). Although TpT seems to adsorb to the CdS particles more strongly, the photodimer quenches the luminescence to a greater degree. We propose that the photodamaged conformation of the dimer makes it more compact; therefore, more of them are able to exchange with the surface Cd^{2+} cations.

However, whereas CdS nanoparticles provide a means for sensitive detection of analyte, photoluminescence provides limited structural information about the adsorbate. SERS compensates for these shortcomings and promises to achieve sensitivities for detection that approach those of photoluminescence.

SERS provides vibrational information about the analytes near the nanoparticles surfaces. For SERS, silver colloids were produced by a seed-mediated growth method as described in the Experimental section. They were characterized by absorption spectroscopy and TEM and tested for SERS activity against the well-documented pyridine spectra [23]. The average Ag colloid diameter was $\sim 44 \pm 4$ nm in all experiments. The particle

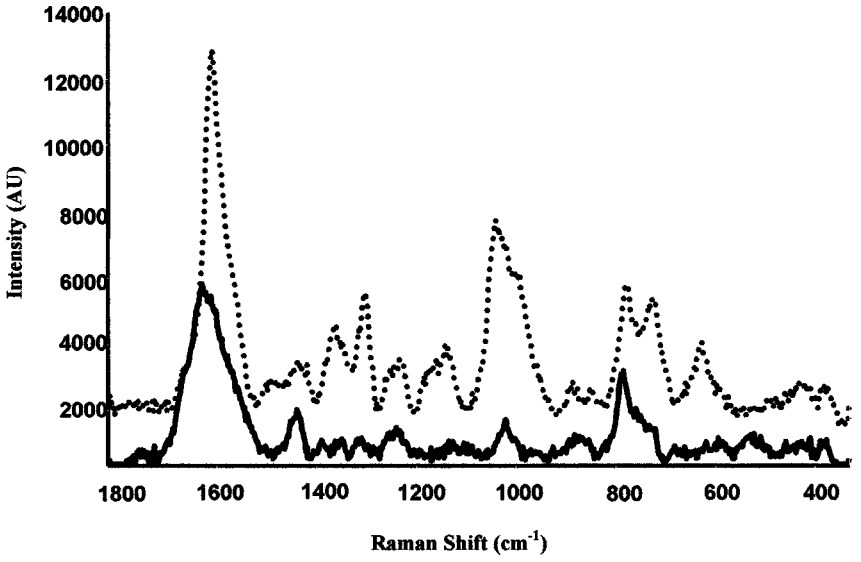

Fig. 7. SERS of 7×10^{-5} M *cis-syn* thymine dimer (dashed line) and TpT (solid line).

aggregation required to optimize the SERS signal was achieved through the addition of KCl.

The Raman spectrum and SERS spectrum of thymine's free base are well documented [35–38]. However, when the sugar and phosphate of a DNA nucleotide are added to thymine, the normal Raman spectrum of the resultant crystalline thymidine monophosphate (TMP) becomes very weak. Similarly, crystalline TpT does not produce a distinct Raman spectrum. However, SERS of TpT in water, with Ag nanoparticles, reveals a vibrational spectrum of TpT at comparatively low concentrations (7×10^{-5} M), indicating a Raman signal enhancement factor of $\sim 10^5$–10^6 that is due to the presence of the metal nanoparticles.

The spectra in Fig. 7 demonstrate distinct differences between TpT and its *cis-syn* dimer. To the best of our knowledge, this is the first SERS spectra of the *cis-syn* thymine photodimer. First, the cyclobutane ring gives rise to a peak around 1000 cm^{-1} in the dimer spectrum [39]. Second, the broad peak of TpT around 1600 cm^{-1} becomes much more defined in the spectrum of the *cis-syn* dimer due to the disappearance of the band at 1656 cm^{-1}, which is characteristic of a C═C double bond [39]. The sharpened band at 1600 cm^{-1} is associated with a C═O stretch and is likely to be enhanced, not only because of the disappearance of the peak associated with the 5,6 double bond, but also because of surface orientation factors [39]. The plausibility of this hypothesis is supported by the conformational changes of the molecule associated with this lesion. The *cis-syn* dimer is more polar than TpT, as is demonstrated by its quicker elution on the HPLC reversed-phase column. A reasonable explanation for this increased polarity is the "tucking" of the methyl groups inward and the effectively forced exposure of the sugar-phosphate backbone (Fig. 8). This suggests a scenario in which these photodamaged molecules adsorb in such a manner at the Ag particle's surface that they experience large electric field enhancements. The lowest concentration of photodimer that we have detected was 1×10^{-5} M; however, methodological improvements will lower this detection limit. However, until SERS matches the detection limits of fluorescence, the two methods complement each other as part of a unified sensing scheme.

In conclusion, there is a clear difference in luminescence quenching of CdS between TpT and its photodimer. The photodimer seems better able to displace "activating" Cd^{2+} at the CdS nanoparticles' surface, thus enabling it to quench the luminescence more completely than the less polar TpT. SERS provides structural, orientational, and possibly molecular conformational information about both analytes. The spectra suggest that the more polar photodimer, as shown in part by its increased signal intensity, adsorbs to the surface of the silver particles in a different orientation. Given the photodimer's increased polarity, as is evidenced by its early elution on a nonpolar column, documentation that its presence distorts DNA by 30°, its CD spectra, and its preference for adsorbing to both CdS and Ag particles, its distorted molecular conformation is further suggested. It is interesting to note that in other work done in our lab, 5′-methylated cytosines in hairpin triplet repeats of *d*(^{m}C^{m}CG) had a noticeably reduced quenching of luminescence compared with the unmethylated d(CCG) repeat, analogous to TpT and its *cis-syn* photodimer [17]. Both fluorescence spectra and SERS suffer limitations,

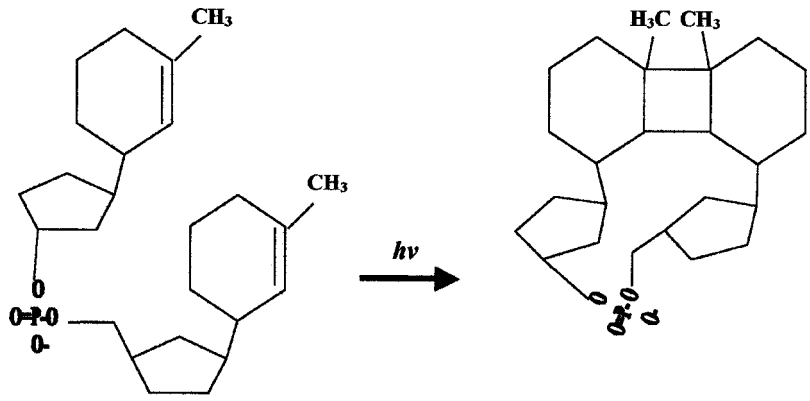

Fig. 8. Possible deformation conformation of the *cis-syn* photodimer showing the tucking of the methyl groups.

but by combining their strengths—the sensitivity of fluorescence and the "fingerprinting" of SERS—using the unique properties of CdS and Ag nanoparticles, low detection limits with improved structural and orientational information of biological analytes are possible and, in our case, provide a clearer picture of how DNA binds to curved surfaces.

REFERENCES

1. P. Catasti, X. Chen, S. V. S. Mariappan, E. M. Bradbury, and G. Gupta (1999). DNA repeats in the human genome. *Genetica (The Hague)* **106**, 15–36.
2. X. Chen, S. V. S. Mariappan, P. Catasti, R. Ratliff, R. K. Moyzis, A. Laayoun, S. S. Smith, E. M. Bradbury, and G. Gupta (1995). Hairpins are formed by the single DNA strands of the fragile-X triplet repeats—Structure and biological implications. *Proc. Natl. Acad. Sci. U.S.A.* **92**, 5199–5203.
3. R. D. Wells and S. C. Harvey (Eds.) (1988). *Unusual DNA Structures*, Springer-Verlag, New York.
4. R. R. Sinden (1994). *DNA Structure and Function*, Academic Press, San Diego, CA.
5. A. P. Wolffe and H. R. Drew (1995). In S. C. R. Elgin (Ed.), *Chromatin Structure and Gene Expression*, IRL, Oxford, pp. 27–48.
6. C. R. Calladine and H. R. Drew (1997). *Understanding DNA*, Academic Press, San Diego, CA.
7. H. Park, K. J. Zhang, Y. J. Ren, S. Nadji, N. Sinha, J. S. Taylor, C. H. Kang (2002). Crystal structure of a decamer containing a *cis-syn* thymine dimer. *Proc. Natl. Acad. Sci. U.S.A.* **99**, 15965–15970.
8. S. Y. Wang (1976). *Photochemistry and Photobiology of Nucleic Acids: Vol. I, Chemistry*, Academic Press, New York.
9. T. Douki, M. Court, F. O. Sauvaigo, and J. Cadet (2000). Formation of the main UV-induced thymine dimeric lesions within isolated and cellular DNA as measured by high performance liquid chromatography-tandem mass spectrometry. *J. Biol. Chem.* **275**, 11678–11685.
10. I. Husain, J. Griffith, and A. Sancar (1988). Thymine dimers bend DNA. *Proc. Natl. Acad. Sci. U.S.A.* **85**, 2558–2562.
11. J. J. Storhoff, R. Elghanian, R. C. Mucic, C. A. Mirkin, and R. L. Letsinger (1998). One pot colorimetric differentiation of polynucleotides with single base imperfections using gold nanoparticle Probes. *J. Am. Chem. Soc.* **120**, 1959–1964.
12. C. J. Murphy and R. Mahtab (2000). Detection of unusual DNA structures with nanoparticles. *Proc. SPIE* **3924**, 10–16.
13. R. Mahtab, J. P. Rogers, and C. J. Murphy (1995). Protein-sized quantum-dot luminescence can distinguish between "Straight," "Bent," and "Kinked" oligonucleotides. *J. Am. Chem. Soc.* **117**, 9099–9100.
14. R. Mahtab, J. P. Rogers, C. P. Singleton, and C. J. Murphy (1996). Preferential adsorption of a "Kinked" DNA to a neutral curved surface: Comparisons to and implications for nonspecific DNA-protein Interactions. *J. Am. Chem. Soc.* **118**, 7028–7032.
15. C. J. Murphy, E. B. Brauns, and L. Gearheart (1997). Quantum dots as inorganic DNA-binding proteins. *Mat. Res. Soc. Symp. Proc.* **452**, 597–600.
16. R. Mahtab, H. H. Harden, and C. J. Murphy (2000). Temperature- and salt-dependent binding of long DNA to protein-sized quantum dots: Thermodynamics of "Inorganic Protein"-DNA interactions. *J. Am. Chem. Soc.* **122**, 14–17.
17. L. Gearheart, K. K. Caswell, and C. J. Murphy (2001). Recognition of hypermethylated triplet repeats in vitro by cationic nanoparticles. *J. Biomed. Opt.* **6**, 111–115.
18. K. Kneipp, H. Kneipp, I. Itzkan, R. R. Dasari, and M. S. Feld (1999). Ultrasensitive chemical analysis by Raman spectroscopy. *Chem. Rev.* **99**, 2957–2976.
19. W. E. Doering and S. Nie (2002). Single-molecule and single-nanoparticle SERS: Examining the roles of surface active sites and chemical enhancement. *J. Phys. Chem. B* **106**, 311–317.
20. J. A. Creighton (1983). Surface Raman electromagnetic enhancement factors for molecules at the surface of small isolated metal spheres—The determination of adsorbate orientation from SERS relative intensities. *Surf. Sci.* **124**, 209–219.
21. A. Campion and P. Kambhampati (1998). Surface-enhanced Raman scattering. *Chem. Soc. Rev.* **27**, 241–250.
22. R. L. Garrell (1989). Surface-enhanced Raman-spectroscopy. *Anal. Chem.* **61**, 401A–411A.
23. M. Moskovits (1985). Surface-enhanced spectroscopy. *Rev. Mod. Phys.* **57**, 783–826.
24. A. M. Michaels, J. Nirmal, and L. E. Brus (1999). Surface enhanced Raman spectroscopy of individual rhodamine 6G molecules on large Ag nanocrystals. *J. Am. Chem. Soc.* **121**, 9932–9939.
25. K. Kneipp, H. Kneipp, R. Manoharan, I. Itzkan, R. R. Dasari, and M. S. Feld (1998). Surface-enhanced Raman scattering (SERS)—A new tool for single molecule detection and identification. *Bioimaging* **6**, 104–110.
26. K. Kneipp, Y. Wang, H. Kneipp, L. T. Perelman, I. Itzkan, R. R. Dasari, and M. S. Feld (1997). Single molecule detection using surface-enhanced Raman scattering (SERS). *Phys. Rev. Lett.* **78**, 1667–1670.

27. K. Kneipp, H. Kneipp, V. B. Kartha, R. Manoharan, G. Deinum, I. Itzkan, R. R. Dasari, and M. S. Feld, (1998). Detection and identification of a single DNA base molecule using surface-enhanced Raman scattering (SERS). *Phys. Rev. E* **57**, R6281–R6284.
28. S. M. Nie and S. R. Emory (1997). Probing single molecules and single nanoparticles by surface-enhanced Raman scattering. *Science* **275**, 1102–1106.
29. L. A. Gearheart, H. J. Ploehn, and C. J. Murphy (2001). Oligonucleotide adsorption to gold nanoparticles: A surface-enhanced Raman spectroscopy study of intrinsically bent DNA. *J. Phys. Chem. B* **105**, 12609–12615.
30. J. E. Yager and C. D. Yue (1988). Evaluation of the xenon arc lamp as a light source for aquatic photodegradation studies—Comparison with natural sunlight. *Environ. Toxicol. Chem.* **7**, 1003–1011.
31. L.-S. Kan, L. Voituriez, and J. Cadet (1988). Nuclear magnetic-resonance studies of cis-syn, trans-syn, and 6-4 photodimers of thymidylyl(3′-5′)thymidine monophosphate and cis-syn photodimers of thymidylyl(3′-5′)thymidine cyanoethyl phosphotriester. *Biochemistry* **27**, 5796–5803.
32. G. D. Fasman (1996). *Circular Dichroism and the Conformational Analysis of Biomolecules*, Plenum, New York.
33. S. Schneider, P. Halbig, H. Grau, and U. Nickel (1994). Reproducible preparation of silver sols with uniform particle size for application in surface-enhanced Raman spectroscopy. *Photochem. Photobiol.* **60**, 605–610.
34. P. Atkins (1994). *Physical Chemistry*, 5th ed., Freeman, New York.
35. V. K. Rastogi, C. Singh, V. Jain, and M. A. Palafox (2000). FTIR and FT-Raman spectra of 5-methyluracil (thymine). *J. Raman Spectrosc.* **31**, 1005–1012.
36. C. Otto, T. J. J. van den Tweel, F. F. M. de Mul, and J. Greve (1986). Surface-enhanced Raman-spectroscopy of DNA bases. *J. Raman Spectrosc.* **17**, 289–298.
37. E. Koglin, J. M. Sequaris, J. C. Fritz, and P. Valenta (1984). Surface-enhanced Raman-scattering (SERS) of nucleic-acid bases adsorbed on silver colloids. *J. Mol. Struct.* **114**, 219–223.
38. R. Aroca and R. Bujalski (1999). Surface enhanced vibrational spectra of thymine. *Vibrational Spectrosc.* **19**, 11–21.
39. F. R. Dollish, W. G. Fateley, and F. F. Bentley (1974). *Characteristic Raman Frequencies of Organic Compounds*, Wiley, New York.